

COMPLETE TEST RESULTS OF NEW BPM ELECTRONICS FOR THE ESRF NEW LE-RING

B.K. Scheidt, ESRF, Grenoble, France

Abstract

Among the 320 BPMs in the ESRF new low-emittance ring, a set of 128 units will be equipped with new electronics, while the other set (192) will be served by the existing Libera-Brilliance electronics. These new electronics are an upgraded version of the low-cost Spark electronics originally developed 3 years ago for the ESRF's injector complex. All these 128 units have been installed in the first half of 2018 on existing BPM signals (through duplication with RF-splitters) and subsequently been tested thoroughly for performance characteristics like stability, resolution and reliability. It shows that while these Sparks have a very straightforward and simple concept, i.e. completely omitting calibration schemes like RF-cross-bar switching, pilot-tone introduction or active temperature control, they are fully compatible with all the beam position measurement requirements of this new ring.

OVERVIEW OF THE BPM SYSTEM

The BPM system in this new storage ring will be a hybrid type with both two types of BPM-block geometries, and two types of BPM electronics. The lattice parameters of the new ring are given in Fig. 1 that represents one complete cell out of the total of 32, with the 10 BPMs indicated in triangles.

The Fig. 2 shows some numeric details of that lattice, the distribution in a cell of the large and the small geometry, and the distribution of the 2 types of electronics.

For the latter we will use a) 192 Liberas that were bought nearly 10 years ago and b) 128 newly developed and procured Sparks. [1]

The old storage ring with 224 BPMs is served with an equal number of Libera-Brilliance units with satisfactory performance and reliability over these 10 years and therefore the logical choice would have been to procure more of them to make-up for the new total number of 320 BPMs. [2]

However, these units had become obsolete. In looking for a satisfactory alternative, we have turned towards a different device that was developed, 3 years earlier, for new Booster BPMs. These relatively simple, straight-forward and of moderate cost Spark electronics offered enough scope for upgrading in order to make them comply with our overall BPM needs and requirements of this new storage ring. [3, 4]

By re-using 192 Libera units out of the 224 presently active units we have increased our cover for spares.

These two different electronics provide data-streams, and buffers with identically synchronised sampling-rates. However, the Fast-Orbit-Correction will only use the 10 kHz stream provided by the 192 Liberas. [5]

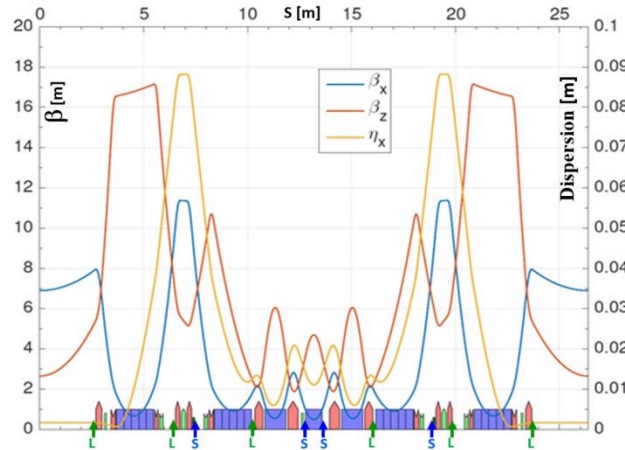


Figure 1: The lattice of one complete cell with the 10 BPM positions indicated by blue/green triangles

BPM	Geom.	Libera/Spark	S [m]	β Hor [m]	β Vert [m]	Disp.[cm]
1	Large	Libera	2.65	7.92	5.30	0.2
2	Large	Libera	6.48	9.50	7.17	8.0
3	Large	Spark	7.52	7.82	6.54	7.3
4	Small	Libera	10.29	1.93	2.33	1.3
5	Small	Spark	12.73	1.13	3.39	1.5
6	Small	Spark	13.64	1.13	3.39	1.5
7	Small	Libera	16.08	1.93	2.33	1.3
8	Large	Spark	18.86	7.82	6.54	7.3
9	Large	Libera	19.90	9.50	7.17	8.0
10	Large	Libera	23.72	7.92	5.30	0.2

Figure 2: The BPM geometry and the type of electronics.

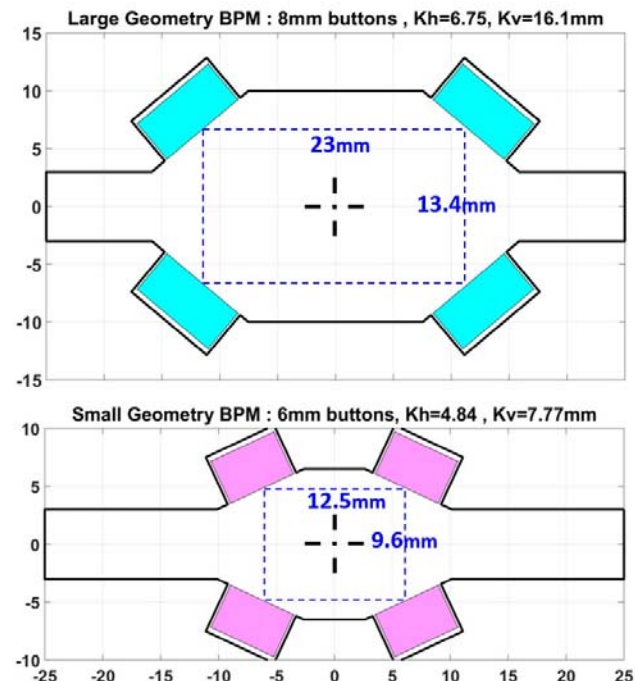


Figure 3: The distinct geometries of the two BPM blocks.

Content from this work may be used under the terms of the CC BY 3.0 licence (© 2018). Any distribution of this work must maintain attribution to the author(s), title of the work, publisher, and DOI.

BPM-buttons and BPM-block Geometries

The geometry of the 2 distinct BPM-blocks are given in Fig. 3 with the large aperture (for BPMs 1,2,3 and 8,9,10) in the top of the figure, and below the small aperture (for BPMs 4,5,6,7). The latter one uses 6 mm diameter BPM-buttons while the large version has an 8 mm diameter. [6]

The Kh and Kv constants, for calculating beam positions in the centre of the block with the simple delta-over-sum calculation, are also indicated and it is to be noted that the large BPM has a particular high (i.e. unfavourable) Kv (16.1 mm) which is due to the unavoidable constraints imposed by the chamber's profile design.

The sensitivity of these buttons at the ESRF's 352.2 MHz frequency is respect. 398 and 352 nV/mA rms for the small and the large geometry. The RF cables, taking these signals to the electronics in one cubicle per cell, will be of a length between 10 and 24 m for the large majority of the 32 cells. These RF-cables (0.2 dB/m loss at 352 MHz) will in fact have four separate RF cables (per BPM station), but bundled in a single jacket with additional shielding.

Characteristics of the New Spark Electronics

In comparison to the original and simple Spark device developed for the Booster 3 years earlier, the upgraded version was modified, or equipped with additional features, as follows :

- Slightly different platform structure & format
- 32 bit processing of all data streams, and result values (integers) in nanometer
- PLL with offset tuning and synchronisation features
- Different RF-amplifiers & SAW filters (and now 2 per channel) due to former obsolete components
- Variable attenuators (32 dB range & 1 dB step) and a calibration scheme to remove offsets.

The RF attenuators are set to limit peak-levels of the ADCs (14bits) to below 4000 counts (half of full-scale). It was found in early prototype tests that some common-mode existed between the A-B and the C-D channels because there are 2 ADCs on a single chip. The resulting degradation of the vertical position resolution was easily resolved by a simple re-arrangement between the 4 channels and the 2 chips. The ADCs are clocked at the ring's orbit frequency by a ratio of 304, i.e. identical to the Liberass, at approx. 108 MHz.

The resolution in beam position shown in Fig. 4 (for a BPM-block with Kh, Kv of 10mm and for CW RF signals) is obtained from factory-acceptance-tests, and expressed for the fastest output rate (Turn-by-Turn, i.e. 355 kHz, BW=170 kHz) and for slow-rate (SA, 40 Hz, BW=16 Hz). Only values for low & moderate beam currents (0.3 to 30 mA) are shown here, together with the corresponding RF-input levels, ADC-counts and attenuator settings.

These values do not use the Spark's possibility of an extra 6 dB gain by switching the ADCs to high-sensitivity; a feature that will serve during the initial ring commissioning at very low-current in T-b-T mode. Also, the time-domain processing feature will then be used that

uses an ADC-mask precisely positioned on only the RF-signal of injected beam, avoid smearing between turns as with the classical T-b-T filter chain.

ADC [cnts]	Att. [dB]	Input [dBm]	Current [mA]	Resolution T-b-T rate [um]	Resolution SA-rate (40Hz) [nm]
3000	10 .. 31	> -30	> 25	< 0.3	< 10
3000	5	-35	15.4	0.44	11
3000	0	-40	8.7	0.72	13
1687	0	-45	4.9	1.27	16
949	0	-50	2.7	2.26	27
533	0	-55	1.5	4.01	39
300	0	-60	0.9	7.14	73
169	0	-65	0.5	12.7	117
95	0	-70	0.3	22.7	209

Figure 4: BPM rms resolution versus beam current.

SIX MONTHS TESTING WITH BEAM SIGNALS ON 4 PARALLEL UNITS

The delivery of the (total of 145) Spark units covered a period from February to April, and the ESRF had decided to install, operate and subsequently test permanently as many units as possible. This was done, up to now (end-August) on 128 units, being installed in groups of 4 parallel units per cell, being fed with RF-signals from an existing BPM, through the use of a set of four 2-way-splitters and four 4-way-splitters per cubicle (cell), as shown in Fig. 5. The 4th BPM in each of the 32 cells was used for this while this BPM station, through its Libera, continued to serve for orbit control, both fast and slow.

Each Spark has also the mechanical support, the timing & trigger signals, and the network connections in place as needed for the commissioning of the ring in early 2020. Moreover, this arrangement allowed developing and verifying the communication and software aspects, both at the lower level (device server) and for higher levels and applications.

In addition to gaining considerable time by progressing with all the installation and preparation work, the 2nd main advantage of this scheme was a rigorous and long-term testing of the stability and reliability of these Spark devices since the essential data was available (during ESRF normal operation) and also stored in our computer data-base for later detailed off-line verifications.

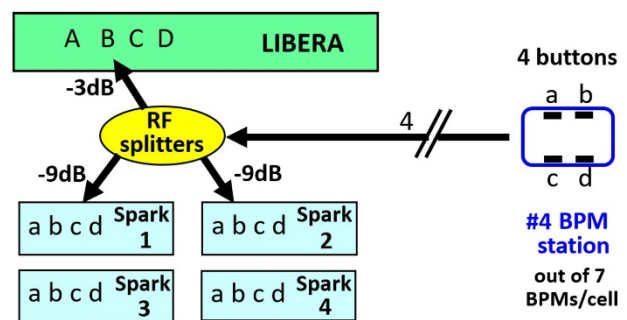


Figure 5: The set-up of testing 4 Sparks on BPM signals.

Drift, Stability and Reproducibility Tests of The Sparks over Short and (Very) Long Periods

It is recalled here that the Spark device is basically a 4 channel digitizer for RF-signals, without any active calibration or compensation scheme. In other BPM electronics such a scheme aims at keeping the 4 sensitivities of each channel equal, typically $< 1E-4$ rms (relative variation) which would correspond to 0.5 μm rms positional stability in a BPM system (for $K=10$ mm). Instead, the Spark relies on an intrinsic stability of its 4 channels, obtained by a careful and compact design, with the absence of internal ventilators. Verifications of this important stability requirement on a few prototypes had been successful. However, the remaining challenge was to now satisfy this requirement: a) in numerous units (>100), and b) over much longer time-scales than obtained with a typical laboratory set-up.

The performance in terms of resolution, for short lengths of measurements (i.e 1 ms to 1 sec) had already been verified on the prototypes, and were found to be excellent and better than those from the Libera-Brilliance units. [7]

The noise value of 10 nm rms on the SA-stream (see Fig. 4) applies for a 1 sec measurement time. The described test configuration of (up to) 32 x 4 Sparks allowed us to now measure this same value (now better qualified as drift) for measurement times from minutes up to months.

The general method was to detect any deviation (in H & V position data, with $K=10$ mm) between each of the 4 units, being themselves in strict parallel & identical conditions. The RF-splitters themselves are supposed without any drift, and so any deviation (drift) detected is attributed to the Spark devices. The initial position offsets (at T_0) of each on the 4 units were removed, with rms drift recorded from then on.

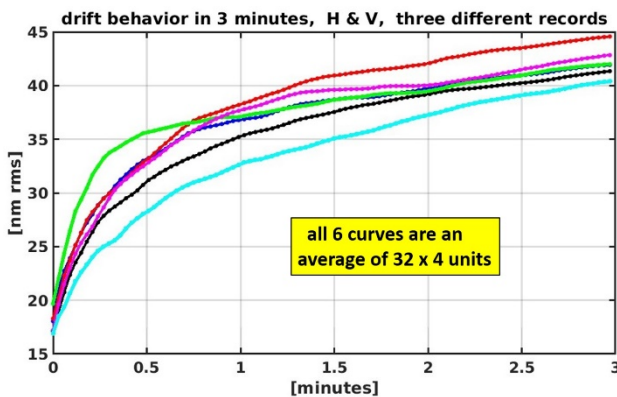


Figure 6: Drift evolution in a 3 minutes period.

Figures 6 and 7 show this drift behaviour over periods of respect. 3 minutes and 6 hours. A total of 6 curves are shown, to simply illustrate that such behaviour is not strictly identical or very reproducible. However, to be noted are the small values: after 3 minutes the rms drift is below 45 nm and after 6 hours below 200 nm.

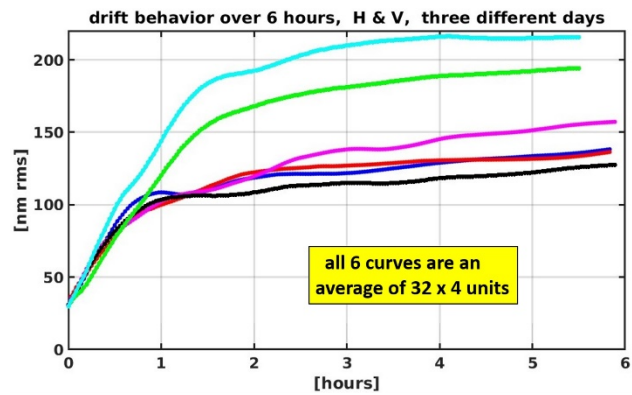


Figure 7: Drift evolution over 6 hours.

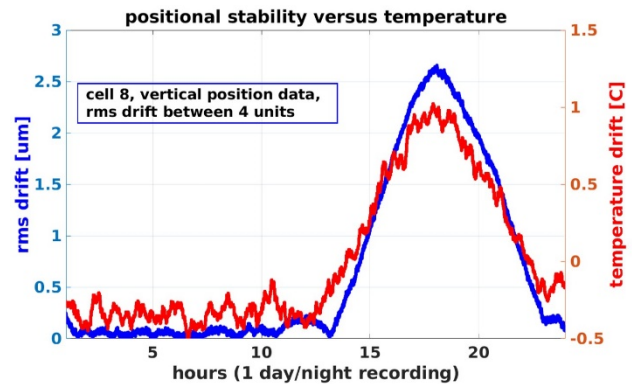


Figure 8: Temperature dependence during 24 hrs period.

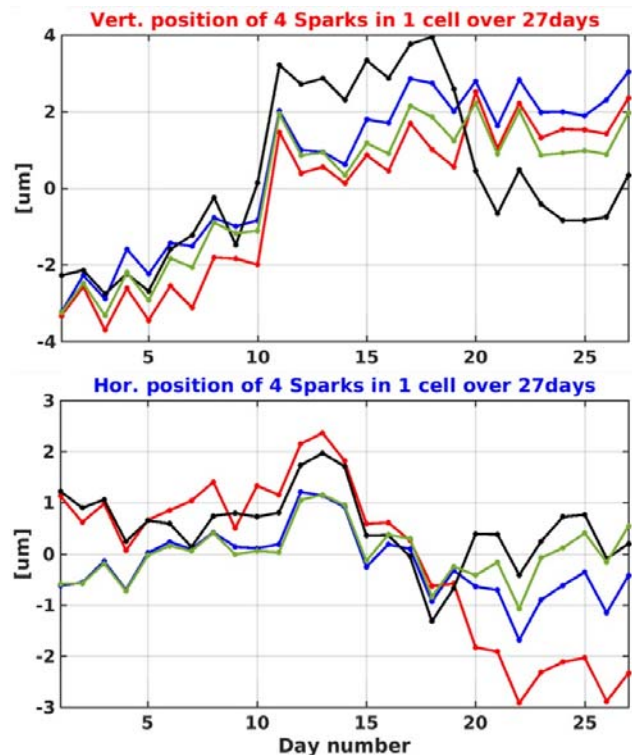


Figure 9: Stability of 4 Sparks over 27 days, top-graph: vertical position, lower-graph: horizontal position.

Assessing this drift over a (continuous) period of much longer than 6 hours was not possible since the temperature stability in our present cubicles is rather poor. The Sparks are affected by it as can be seen in Fig. 8: The temperature rises in afternoon by about 1.3 °C and the rms drift between the 4 units rises correspondingly to about 2.6 μm . This is compatible with the device specifications of $<3 \mu\text{m}/^\circ\text{C}$. We will improve the cubicle's global temperature control in the future, and notably suppress this strong 24 hrs fluctuation.

To effectively assess that drift now over longer periods, e.g. one month, we took the H & V position data at each day on an average of data within 1 hr of stable temperature (typically taken in the night). The Fig. 9 shows the stability over 27 days of 4 such Sparks in one cubicle. The curves show a) some common variation (attributed to motion of the beam in that common BPM) and b) the non-common part that can be attributed to drifts of the Sparks.

The rms value of the 4 position values, both hor. and vert. is calculated, but now on 24 such cells (i.e. 96 Sparks) and shown in Fig. 10. The conclusion is that the average stability over a 24 days period is below 1 μm .

Drift versus beam current was also assessed and found to be below 1 μm for $>50\%$ variation of beam current.

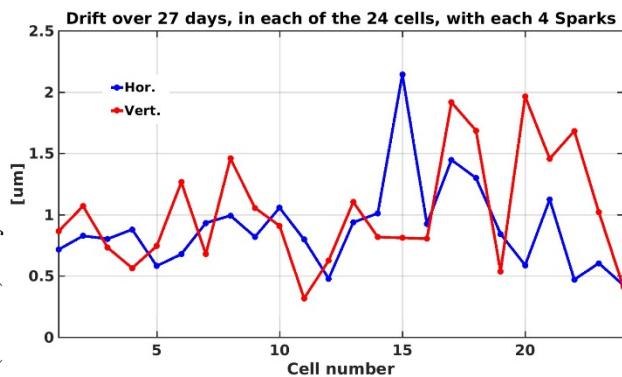


Figure 10: Drift rms over 24 days on 24 x 4 BPM stations.

SOFTWARE AND OTHER TOPICS

The devices include a Tango interface provided by the company, with the source code available to our ESRF software engineers, allowing modifications and the implementation of position calculations based on polynomial approximations. The latter are more accurate than the ordinary delta-over-sum (dos) algorithm.

We did the assessment of such polynomial-based calculation on the embedded dual core ARM processor of the unit. It offers very good performances for double precision floating point arithmetic, with up to 700K positions calculations per second using a seventh order, 2 dimensional polynomial. This speed is sufficient for the 40 Hz real time stream and to yield triggered buffers without problems or any noticeable extra delay.

The simulations done with boundary-element methods have shown that the dos formula is strongly un-precise, for both BPM geometries, even for moderate displacements from the BPM centre. The same tool (Bpmlab) used for these simulations also allows the calculation of a suitable set of polynomials. [8]

These polynomials and their coefficients, with different sets for the two BPM geometries, are conveniently uploaded into the above software. When selected, under Tango control, they provide the beam coordinates with much higher accuracy even for a strongly off-centred ($>10\text{mm}$) beam position as can be expected during the beam trajectory studies at the initial commissioning period of this new ring.

However, for the fast orbit control, the 10 kHz FA-data-stream (provided by the 192 Libera-brilliance units only), will only use the dos algorithm as before.

CONCLUSION

We tested a large number of Spark BPM electronics simultaneously and for many months under situations and conditions comparable to normal use for beam orbit control, i.e. with real BPM input signals, corresponding timing & clock signals, and with full integration into the computer network. The results are very satisfactory in terms of resolution, stability and reproducibility, also concerning the overall reliability of this device. We thereby demonstrated that this Spark, characterised by a careful design that omits complexity, can fully satisfy the orbit measurement requirements of the ESRF's new low emittance ring from 2020 onwards.

ACKNOWLEDGEMENTS

The author would like to thank the colleagues in the ACU-unit, and notably J-L.Pons, for the smooth integration of these devices in the ESRF control & computer system. Colleagues in the Diagnostics group have also been very helpful, and notably F.Taoutaou, for the physical installation, connectorization and configuration of the devices and all the RF cables & components in the cubicles.

REFERENCES

- [1] Instrumentation Technologies, <https://www.i-tech.si/>.
- [2] K.Scheidt, "Installation and commissioning of a complete upgrade of the BPM system for the ESRF Storage Ring", in *Proc. DIPAC'09*, paper MOPD05.
- [3] K.Scheidt, "First results with the prototypes of new BPM electronics for the Booster of the ESRF", in *Proc. IBIC'14*, paper TUPF15.
- [4] M.Cargnelutti, "Commissioning results of the new BPM electronics of the ESRF Booster", in *Proc. IPAC'15*, paper MOAB3.
- [5] E.Plouviez, "The orbit correction scheme of the new EBS of the ESRF", in *Proc. IBIC'16*, paper MOPG09.
- [6] K.Scheidt, "Newly developed Buttons for the BPMs in the ESRF Low-Emittance Ring", in *Proc. IBIC'14*, paper TUPF14.
- [7] K.Scheidt, presentations at Libera and DEELS workshops in 2015, 2016.
- [8] A. A. Nosych, U. Iriso, J. Olle, "Electrostatic finite-element code to study geometrical nonlinear effects of BPMs in 2D", in *Proc. IBIC'15*, paper TUPB047.